Scientific Reports

https://doi.org/10.1038/s41598-026-40607-2

Article in Press

Structural stability of symmetric bispecific antibodies: a case study showing potential compromise near linker regions

Received: 29 June 2025

Accepted: 13 February 2026

Published online: 18 February 2026

Cite this article as: Ingavat N., Kok Y.J., Dzulkiflie N. *et al.* Structural stability of symmetric bispecific antibodies: a case study showing potential compromise near linker regions. *Sci Rep* (2026). https://doi.org/10.1038/s41598-026-40607-2

Nattha Ingavat, Yee Jiun Kok, Nuruljannah Dzulkiflie, Liew Jia Min, Wang Xinhui, Kia Ngee Low, Ka Pui But, Amihan Anajao, Loh Han Ping, Han Kee Ong, Farouq Bin Mahfut, Yuansheng Yang, Xuezhi Bi & Wei Zhang

Structural Stability of Symmetric Bispecific Antibodies: A Case Study Showing Potential Compromise Near Linker Regions

Nattha Ingavat[1*], Yee Jiun Kok[2*], Nuruljannah Dzulkiflie[1], Liew Jia Min[1], Wang Xinhui[1], Kia Ngee Low[2], Ka Pui But[2], Amihan Anajao[2], Loh Han Ping[3], Han Kee Ong[3], Farouq Bin Mahfut[3], Yuansheng Yang[3], Xuezhi Bi[2**], and Wei Zhang[1**]

[1] Downstream Processing Group, Bioprocessing Technology Institute (BTI), Agency for Science, Technology and Research (A*STAR), Singapore, 138668, Republic of Singapore

[2] Protein Analytics Group, Bioprocessing Technology Institute (BTI), Agency for Science, Technology and Research (A*STAR), Singapore, 138668, Republic of Singapore

[3] Cell Line Development Group, Bioprocessing Technology Institute (BTI), Agency for Science, Technology and Research (A*STAR), Singapore, 138668, Republic of Singapore

*Authors contributed to the manuscript equally.

** Corresponding authors: zhang_wei@bti.a-star.edu.sg; bi_xuezhi@bti.a-star.edu.sg

Abstract:

Over recent decades, bispecific antibodies (bsAbs) have garnered significant attention for their superior therapeutic efficacy compared to progenitor monoclonal antibodies, enabling innovative treatment strategies. Despite their potential, the development of bsAbs presents significant challenges, with structural stability playing a pivotal role in manufacturability, therapeutic performance, and safety. Among the factors influencing stability, the design and incorporation of molecular linkers are particularly critical. In this study, we investigated the structural stability and fragmentation profiles of a symmetric bispecific antibody (Sym-bsAb), targeting HER2 and CD3, under forced degradation conditions. The Sym-bsAb exhibited pronounced fragmentation under prolonged thermal stress, particularly when combined with high pH and salt conditions. Intact mass analysis identified key degradation events, including sequential clipping along G4S and G4 linkers, fragmentations at interchain cystinyl residues and cleavage at the C-terminal of asparagine residues. The identification of G4S and G4 linkers as vulnerable regions prone to clipping in Sym-bsAb provided valuable insights into the stability and manufacturability of bsAbs incorporating linker sequences, underscoring critical considerations for their development.

Keywords: symmetric bispecific antibodies, G4S linker, G4 linker, structural stability, antibody fragmentation

Abbreviations:

BiTE: bispecific T cell engager

bsAbs: bispecific antibodies

Fab: Fragment antigen-binding

HCCF: Harvest cell culture fluid

H: Heavy chain

HMW: high molecular weight species

HPLC-SEC: High-performance liquid chromatography-size exclusion chromatography

L: Light chain

LMW: low molecular weight species

mAb: monoclonal antibody

Sym-bsAb: symmetric bispecific antibody

$(V_H)_{scFv}$: Variable heavy chain of a single-chain fragment

$(V_L)_{scFv}$: Variable light chain of a single-chain fragment

1. Introduction

Bispecific antibodies (bsAbs) have emerged as promising next-generation biologic drugs for clinical use, with their demand increasing significantly over the past decades. Being able to recognise two targets in cis or trans orientation, BsAbs provide enhanced efficacy and enable synergistic treatment mechanisms that cannot be achieved with any combinations of the traditional monoclonal antibodies (mAbs)[1, 2]. Additionally, bsAbs address issues of drug resistance, further enhancing their therapeutic potential[3, 4]. Reflecting their rising demand, the global market size for bsAbs reached 8.5 billion USD in 2023[5], with a projected compound annual growth rate (CAGR) of 34.8% from 2023 to 2030[6].

There are more than 100 different bispecific antibody formats reported thus far[7, 8]. All of these formats can be broadly classified into three main categories: fragment-based, asymmetric, and symmetric bsAbs[3, 9, 10]. Fragment-based bsAbs are the simplest, consisting only of antigen-binding domains and linkers without the Fc region. Blinatumomab, nested under the fragment-based BiTE (bispecific T-cell engager) format, is the first commercial bsAb molecule approved by FDA in 2014[11]. In contrast, both asymmetric and symmetric bsAbs contain the Fc region. Asymmetric bsAbs typically comprise up to four polypeptide chains (heavy chains and light chains) derived from two different mAbs, while symmetric bsAbs are designed to avoid chain association issues and are typically structured as tetravalent (2+2) molecules. Asymmetric bsAbs are available in various sub-formats, such as Roche's Vanucizumab (RG7221) and Faricimab[3, 7] which are prominent CrossMAb examples, and Zanidatamab is the first asymmetric bsAb under Fab-scFv-Fc format to be approved by FDA in November 2024[12].

The symmetric format of bispecific antibodies was first introduced in 1997 as an alternative design to address chain-association issues while retaining the Fc region[10]. This format includes fragment-based configurations that are fused via linkers to either the Fc domain or a conventional antibody (IgG), as well as modified IgGs engineered to recognize two distinct antigens[7, 10]. Over time, symmetric bsAbs have emerged as a highly attractive configuration for therapeutic applications. Two IgG(H)-$(scFv)_2$, Cadonilimab[13] and Ivonescimab[14], are available as commercial products, while several others are currently undergoing clinical studies[7, 15, 16]. For symmetric bsAbs, peptide

linkers are often employed for their structural assembly. Optimizing the composition and length of these linkers is critical to ensure molecular stability and functional performance[7].

Figure 1 depicts a previously engineered model symmetric bispecific antibody (Sym-bsAb)[17] comprising two pairs of polypeptide chains)[18]: (i) a standard trastuzumab light chain (L: V_LC_L) and (ii) a modified heavy chain incorporating an anti-CD3 scFv within the trastuzumab heavy chain (H: V_H-C_{H1}-scFv-Fc/2) connected by three glycine/serine-rich linkers. The G4S linker serves dual functions: as an interdomain linker (Linker 1) between the Fab and scFv domains and as intradomain linker (Linker 2: $(G4S)_3$) connecting the V_H and V_L components within the scFv domain, while a G4 linker (Linker 3) connects the scFv and Fc domains. G4S linker is widely used both within the scFv domain and in scFv-containing bsAbs, including the commercial BiTE, Blinatumomab[3]. Our linker design for Sym-bsAb, including the type and length of amino acids, was guided by previous studies indicating that a linker length longer than 12 amino acids could enable the covalently concatenated V_L and V_H to form highly monomeric and functional scFv[19]. In contrast, shorter linkers, 4 to 5 amino acids, are used to interlink two domains (e.g. linking the scFv domain to the Fab or Fc domain)[3]. Although the Sym-bsAb demonstrated acceptable binding affinity to its target[18], its stability under various stress conditions also plays a vital role in its development and manufacturing.

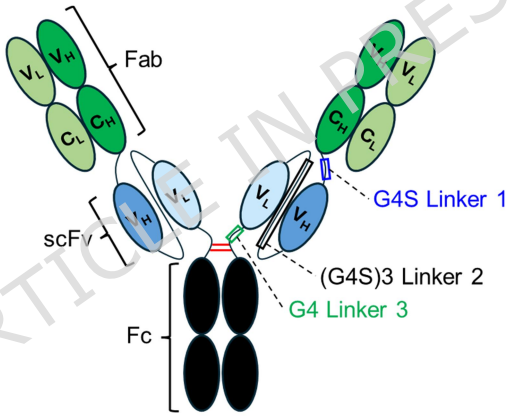

Figure 1. Symmetric bispecific antibody (Sym-bsAb), used as a model for this study, is a symmetric molecule of "2+2" valency with homodimeric wild-type Fc, $(FabscFv)_2$-Fc. G4S Linker 1 connects the Fab domain and the (V_H)scFv domain intermolecularly, $(G4S)_3$ Linker 2 connects the V_H and V_L within the scFv domain intramolecularly, while G4 Linker 3 connects the (V_L)scFv domain to the Fc domain. Abbreviations: Fab = Fragment antigen-binding; (V_H)scFv or (V_L)scFv = Variable heavy or light chain, respectively, of a single-chain fragment variable.

In this study, we demonstrated the structural instability of the Sym-bsAb model molecule (Figure 1) under prolonged thermal stress. Further investigation was carried out to examine the influence of pH and ionic strength—selected based on typical purification and formulation ranges—on Sym-bsAb stability, with potential cleavage sites identified by mass spectrometry (MS) analysis. The detection of degraded Sym-bsAb mass species corresponding to cleavages at G4S and G4 linkers was of

particular concern, as such instability may pose challenges to the development and manufacturability of Sym-bsAb and, potentially, other bsAb formats incorporating these common linkers.

2. Results and Discussion

2.1. Initial investigations on stability of the Sym-bsAb under thermal stress

Following Protein A purification, Sym-bsAb was buffer-exchanged into 50 mM sodium acetate pH 5.5, 250 mM NaCl, and then incubated at elevated temperature of 40 °C. Purity profiles were monitored over 4 weeks using HPLC-SEC.

The HPLC-SEC purity profiles after 4 week-incubation were used to guide peak integration. Figure S1 shows that Sym-bsAb monomer appeared as the main peak (retention time 12.2 - 13.6 min), with high molecular weight species (HMW), and low molecular weight species (LMW). The integration for LMW at the specified retention time (>13.6 min) was performed to account for potential degraded fragments that were not well resolved by HPLC-SEC.

The %Main of Sym-bsAb decreased by 7.2% over the 4-week incubation period (Figure 2A). Concurrently, the %LMW increased by approximately 5%, and the %HMW rose by about 2.3% (Figure 2B). These changes indicate significant degradation of Sym-bsAb under thermal stress conditions. Given our focus on investigating the fragmentation and degradation of Sym-bsAb, we further examined the impact of ionic strength and pH on its fragmentation profiles.

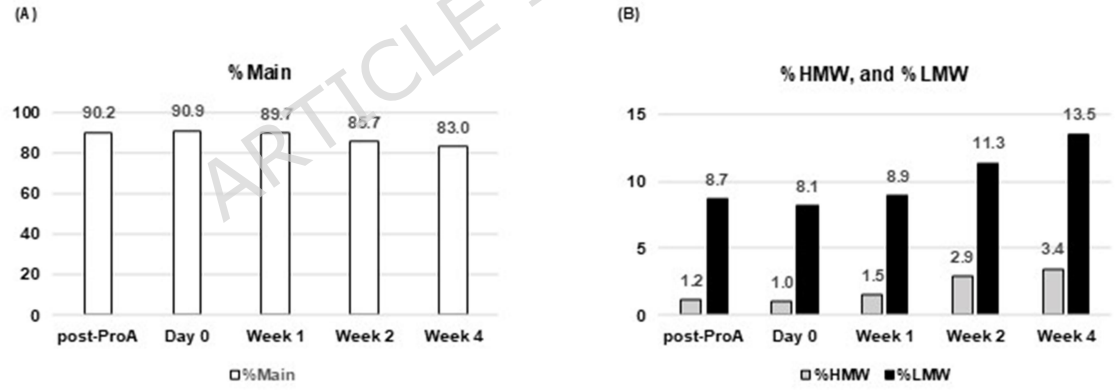

Figure 2. Analysis of protein purity for Sym-bsAb after 4 weeks of incubation in 50 mM sodium acetate (pH 5.5), 250 mM NaCl at 40°C. (A) %Main, (B) %HMW, and %LMW are depicted. %Purity was determined by HPLC-SEC. Post-ProA refers to the Protein A eluate at pH 6.5 prior to buffer exchange.

2.2. Exploration of the influence of ionic strength and pH on fragmentation of Sym-bsAb

To account for changes in purity since the buffer exchange step, we compared the purity profiles of Sym-bsAb in 12 different buffer conditions (50 mM sodium acetate pH 5.5, 50 mM sodium phosphate pH 7.0, and 50 mM Tris pH 8.5 with 0 – 500 mM NaCl) after 40 days of incubation at 40 °C with those of a post-Protein A sample (Figure 3). The change in purity of Sym-bsAb was minimal after

buffer exchange, with %Main values ranging from 89.0% (post-Protein A) to 89.0–91.4% (post-buffer exchange) (Figure S2). However, a decline in Sym-bsAb purity was observed over the 40-day incubation period, with a more pronounced decline in higher pH buffers. This decline in %Main (Figure 3A) was accompanied by an increase in %LMW (Figure 3B) as evidenced by HPLC-SEC, along with more fragments detected on SDS-PAGE (Figure 4), affirming increased fragmentation at higher pH levels.

Interestingly, ionic strength seemed to have a relatively small effect on the Sym-bsAb fragmentation, as evidenced by minimal differences in %LMW at different salt concentrations across each same pH value (Figure 3B). However, the buffer with the highest pH and salt concentration (50 mM Tris, pH 8.5, and 500 mM NaCl) exhibited a significantly higher %LMW compared to other buffers at the same pH of 8.5 but lower salt concentrations (0, 125, and 250 mM NaCl) (Figure 3B, and Figure 4C).

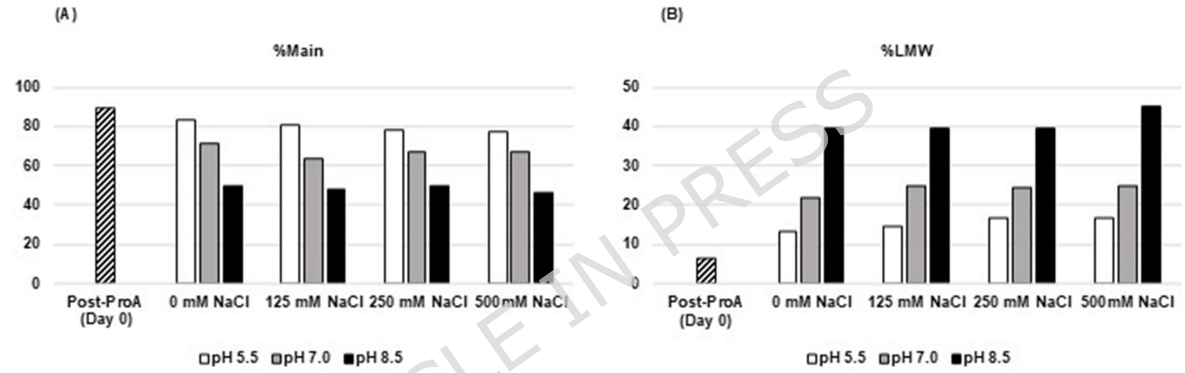

Figure 3. Analysis of Sym-bsAb purity after 40-day incubation at 40°C under various pH (pH 5.5, pH 7.0, pH 8.5) and salt conditions (0 – 500 mM NaCl). (A) %Main and (B) %LMW are depicted. %Purity was determined by HPLC-SEC. Post-ProA refers to Protein A eluate at pH 6.5 prior to buffer exchange.

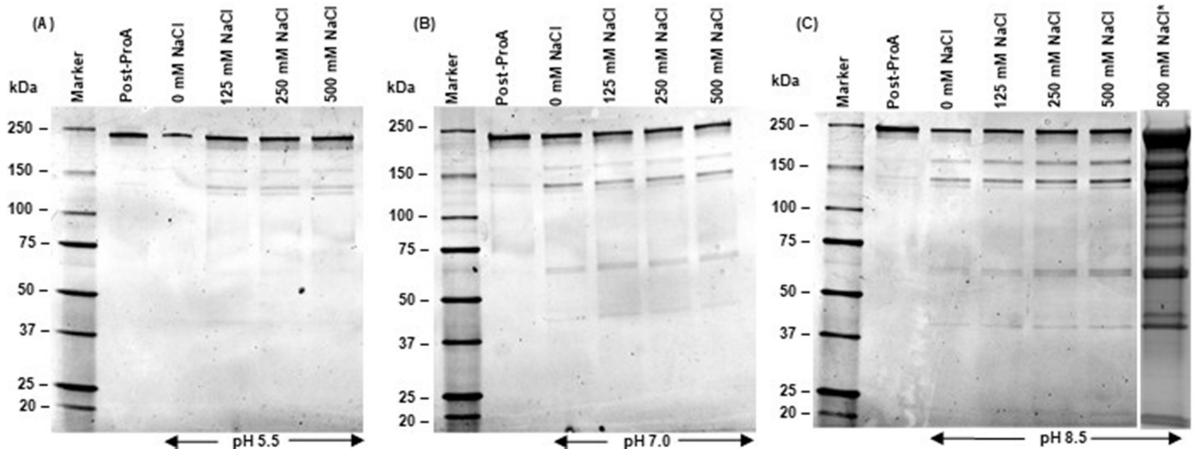

Figure 4. Non-reducing SDS-PAGEs depict protein populations of Sym-bsAb, Post-ProA, and those post-40 day-incubation at 40 °C in buffers with different pH, (A) pH 5.5 (B) pH 7.0 (C) pH 8.5

and salt concentrations (0 – 500 mM NaCl). Approximately 0.3 µg of protein was loaded per lane on the SDS-PAGE, except for the lane marked with (*) which was loaded with ~33 µg of total protein for better visualization of the fragments. Marker units are in kilodaltons (kDa).

Our study demonstrates structural instability of Sym-bsAbs under thermal stress in alkaline conditions. Alkaline environments accelerate chemical modifications and peptide bond cleavages, resulting in structural changes and reduced stability.

Key chemical modifications in alkaline solutions include deamidation of asparagine (Asn) to aspartic acid (Asp), which alters charges and protein conformation[20]. Alkaline stress also promotes peptide bond cleavages, such as Gly-Gly cleavage due to minimal steric hindrance. Beta-elimination of disulfide bonds leads to fragmentation[21], while hydroxyalkyl side chains of serine (Ser) and threonine (Thr) undergo cleavage via intermediates like oxazolidine and ester formations[20]. Additionally, at high pH, deprotonation of acidic residues (Asp and Glu) disrupts stabilizing salt bridges and hydrogen bonds, compromising structural integrity and potentially causing partial unfolding or aggregation. For Sym-bsAb, flexible linker regions (G4S, G4) are likely more exposed, rendering these regions particularly vulnerable to fragmentation[20].

High salt concentrations can synergically promote protein fragmentation, particularly in antibodies susceptible to salt-induced conformational changes. Increased ionic strength destabilizes protein structure[22], inducing partial unfolding and exposing vulnerable regions to proteolysis and chemical modifications. Furthermore, high salt environments can shift the local pH near the protein surface[23], accelerating reactions such as deamidation[24].

2.3. Characterizing stress-induced Sym-bsAb fragments

Mass spectrometry analysis was subsequently conducted to characterize the major Sym-bsAb fragments generated under stress conditions (40°C for 40 days in 50 mM Tris pH 8.5, 500 mM NaCl buffer) which resulted in the most pronounced degradation. To improve detection sensitivity of the various fragmented Sym-bsAb species (Figure 4C), stressed Sym-bsAb was first fractionated using SEC-HPLC. The eluted fractions corresponding to the three distinct elution peaks, Peaks 1, 2 and 3 (Figure 5), were collected and subsequently analyzed by LC-MS.

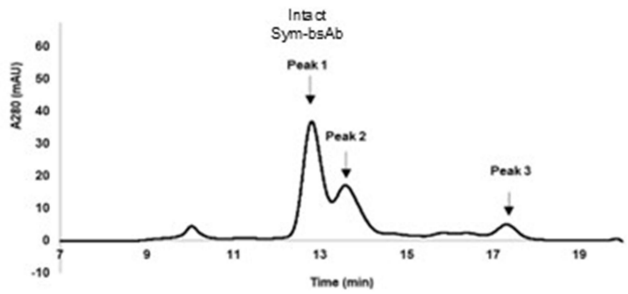

Figure 5. HPLC-SEC chromatograms of the Sym-bsAb sample after a 40-day thermal stress treatment.

2.3.1. Sym-bsAb fragments derived from cleavage of linker sequences

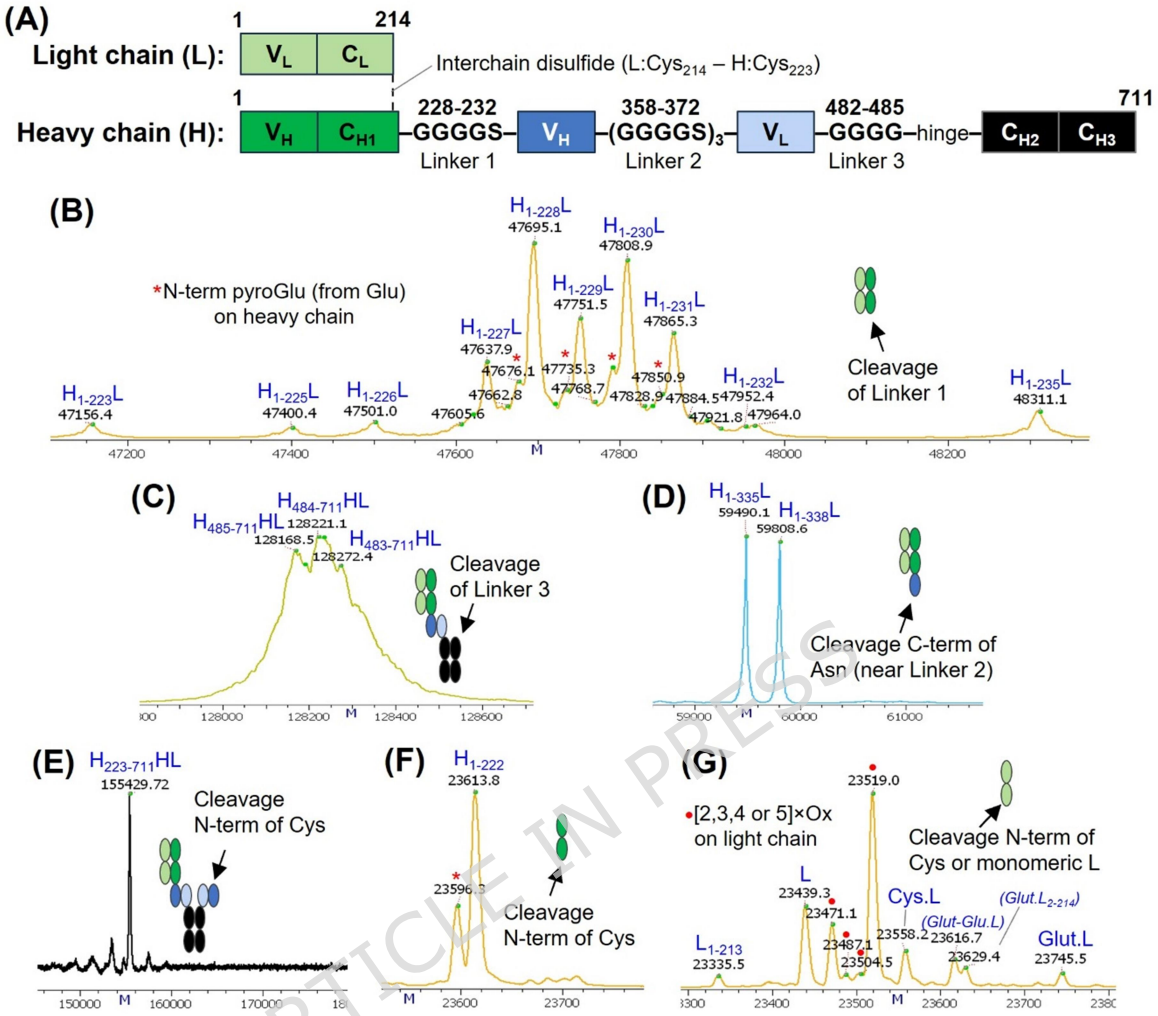

Identity	Fragment region	Clipped sequence	Modification	Observed (Da)	Expected (Da)	Delta (Da)
$H_{1-223}L$	Linker 1	…C|DKTHGGGGSEVQL…	--	47,156.4	47,155.2	1.2
$H_{1-225}L$		…CDK|THGGGGSEVQL…	--	47,400.4	47,398.4	1.9
$H_{1-226}L$		…CDKT|HGGGGSEVQL…	--	47,501.0	47,499.5	1.4
$H_{1-227}L$		…CDKTH|GGGGSEVQL…	--	47,638.0	47,636.7	1.3
$H_{1-228}L$		…CDKTHG|GGGSEVQL…	--	47,695.1	47,693.7	1.4
$H_{1-229}L$		…CDKTHGG|GGSEVQL…	--	47,751.5	47,750.8	0.7
$H_{1-230}L$		…CDKTHGGG|GSEVQL…	--	47,808.9	47,807.8	1.1
$H_{1-231}L$		…CDKTHGGGG|SEVQL…	--	47,865.3	47,864.9	0.5
$H_{1-232}L$		…CDKTHGGGGS|EVQL…	--	47,952.4	47,952.0	0.5
$H_{1-235}L$		…CDKTHGGGGSEVQ|L…	--	48,311.1	48,308.3	2.8
$H_{485-711}HL$	Linker 3	…VLGGG|GDK…	G0F/G0F	128,168.5	128,160.8	7.8
$H_{484-711}HL$		…VLGG|GGDK…	G0F/G0F	128,221.1	128,217.8	3.3
$H_{483-711}HL$		…VLG|GGGDK…	G0F/G0F	128,272.4	128,274.9	-2.4
$H_{1-335}L$	Asn C-terminal (near Linker 2)	…NFGN|SYISY…	--	59,490.1	59,488.8	1.3
$H_{1-338}L$		…N|FGNSYISY…	--	59,808.6	59,807.1	1.5
$H_{223-711}HL$	Cys N-terminal (H-L disulfide)	…EPKS|CDKT…	C_{223}: Cys -> Dha -> Pyruvoyl	155,429.7	155,422.7	7.1
H_{1-222}			S_{222}: C-term amidation	23,613.8	23,614.2	-0.4
L_{1-213}		…KSFNRGE|C	E_{213}: C-term amidation	23,335.5	23,334.7	0.8
L	(monomeric L)	--	--	23,439.3	23,438.8	0.4
L		--	C_{214}: S-Cysteinylation	23,558.2	23,558.0	0.2
L		--	C_{214}: S-Glutathionylation	23,745.5	23,744.1	1.3

Figure 6. Masses and mass-derived structures of intact and fragmented Sym-bsAb species detectable by LC-MS. (A) Sequence structure of Sym-bsAb light and heavy chains, with start and end amino acid positions of polypeptide chains and linker sequences labelled. (B-G) Fragmented Sym-

bsAb masses detected in stressed Sym-bsAb. Masses corresponding to fragments derived from covalent (peptide and disulfide) bond disruptions and chemical degradation (N-terminal pyroGlu and oxidation) were observed. Table insert: Major fragmented mass species are presented in greater detail; truncated heavy (H) or light (L) chains are annotated with a subscript indicating the start and end amino acid positions relative to their respective full-length polypeptides; linker sequences are underlined; Dha – Dehydroalanine; all masses in table are corrected to nearest 1 decimal place.

Intact mass analysis by LC-MS identified fragmented species to be potentially derived from peptide backbone fragmentation events or disruption of intermolecular disulfide bond between the H and L chains (Figure 6). Notably, mass species corresponding to sequential fragmentation along the G4S Linker 1 (~48 kDa species, Figure 6B) and the G4 Linker 3 (~128 kDa species, Figure 6C) were observed, suggesting inherent structural weaknesses of these commonly used flexible peptide sequences that link recognition domains in the engineering of various bsAb formats. Peptide mapping of excised G4S Linker 1 fragments gel band in a preliminary study has supported their identities (Figure S3). Lack of steric hindrance, particularly at Gly-Gly site, has been proposed to facilitate the formation of a tetrahedral intermediate preceding peptide bond hydrolysis under both acidic and basic conditions[20]. No mass species corresponding to fragmentation at Linker 2, however, was identified by LC-MS, though an SDS-PAGE protein band potentially corresponding to Linker 2 N-terminal fragments (faint ~62 kDa band, just below the 75 kDa marker) could be detected (Figure 4C, 33 μg load). Linker 2 is positioned between Linkers 1 and 3, hence Linker 2 fragments could have been further degraded by fragmentation at Linker 1 or 3 sequences, leading to increase heterogeneity and decrease concentration of individual fragment mass species which impacted their detectability; this was corroborated by the detection of only the Linker 1 N-terminal fragments and the Linker 3 C-terminal fragments, i.e. fragments which did not contain other linker sequences that could be further degraded. The higher number of possible cleavage sites along the ~3× longer $(G4S)_3$ Linker 2 would have further exacerbated the heterogeneity and concentration issues. In addition, Linker 2 is also the only linker to connect two interacting subdomains – V_H and V_L, which could have potentially provided some steric shielding to limit degradation.

2.3.2. Sym-bsAb fragments derived from disruption of other bonds (at non-linker sequences)

Mass species arising from fragmentation at C-terminal of Asn residues, and at N-terminal of cystinyl residues, i.e. Cys residues involved in disulfide bonding, were also observed (Figure 6D-G); both fragmentation events are known to occur in mAbs[20]. Asn residue generally undergoes deamidation under alkaline pH, but fragmentation is known to occur if the deamidation reaction has proceeded very slowly, with the rate influenced by the size of the residue C-terminal to Asn or by higher order protein structure[25]. The Asn C-terminal fragment mass species observed corresponded to cleavage at $H:N_{335}$ or $H:N_{338}$ (Figure 6D), which interestingly are also the closest Asn residues to the $(G4S)_3$ Linker 2. The H-L intermolecular disulfide bond is known to be the most susceptible disulfide bond to modifications in mAbs[26], and its proximity to Linker 1 could have exposed the bond further to the environment. Fragmentation N-terminal of cystinyl residues purportedly proceeds by β-elimination of a disulfide bond to form two dehydroalanines (Dha) and subsequent peptide bond

cleavage N-terminal to Dha, with C-terminal amidation and conversion of Dha to pyruvoyl group in the resultant N- and C-terminal fragment species respectively[20]. In the stressed Sym-bsAb sample, all possible mass species corresponding to fragmentation at H-L interchain cystinyl residues could be detected (except for the single Cys fragment derived from cleavage N-terminal to L:C_{214} which is below the defined detection mass range) (Figure 6E-G).

2.3.3. Sym-bsAb mass species corresponding to monomeric light chain moieties

Other major mass species detected by LC-MS corresponded to monomeric L moieties, comprising L chains with an unpaired free Cys residue, or S-cysteinylated/glutathionylated Cys residue (Figure 6G). S-cysteinylated or S-glutathionylated L chains were likely not products of forced degradation as the L chains were expressed in excess of H chains to reduce aggregation[27]; excess L chains are commonly secreted into the culture medium and can be modified by Cys or glutathione present within the cells or the culture medium. L chains with a free Cys residue and varying degree of oxidation (Figure 6G), however, were likely to have formed from disulfide bond reduction during the prolonged stress treatment after buffer-exchange (thus removal of Cys and glutathione), but it is not possible to determine the contribution of bsAb molecules and excess (S-cysteinylated/glutathionylated) L chains to these reduced L chains. Reduction of disulfide bonds in therapeutic antibodies bioprocessing has been reviewed in detail by Ren et al. [28], with root cause attributed to redox enzymes released from lysed cells, as well as physical factors affecting reduction rate and reaction equilibrium, and intrinsic structural factors affecting susceptibility of disulfide bonds to enzymatic reduction.

3. Conclusion

Many symmetric bsAbs have advanced to commercial use or clinical studies. However, our study highlights the pronounced structural instability of the Sym-bsAb molecule under thermal stress, particularly in high salt and pH environments. Intact mass analysis revealed major fragmentations at the interdomain regions of flexible linkers, specifically G4S Linker 1 and G4 Linker 3, underscoring their susceptibility to environmental stress. This instability likely arises from the increased molecular flexibility introduced by the multiple flexible linkers in Sym-bsAb, which may expose proximal regions, making them more vulnerable to fragmentation and chemical modifications.

More broadly, linker vulnerability within bsAbs will also be affected by overall stability of these engineered molecules, which is largely format-specific and influenced by sequence variability. Given the common use of linker sequences to connect functional domains in bsAbs, our findings highlight the critical importance of meticulous design and optimization of linker regions, antibody sequences and architectures to improve bsAb stability.

4. Material and Methods

4.1. Materials

All buffers, salts, and reagents were purchased from Sigma-Aldrich except for disodium hydrogen phosphate, citric acid, histidine hydrochloride, and MES that were purchased from Merck Millipore. MabSelect^{TM} PrismA was purchased from Cytiva.

4.2. BsAb culture production

Symmetric bispecific antibody (Sym-bsAb) was produced by stably transfecting CHO K1 cell lines using site-specific integration of plasmid vectors. These vectors carried genes encoding the trastuzumab light chain, trastuzumab V_H-CH1 coupled to anti-CD3 scFv and linked to Fc. The cDNAs for trastuzumab V_L and V_H, as well as anti-CD3 V_L and V_H, were designed using the amino acid sequences of trastuzumab and pasotuxizumab from the international ImMunoGeneTics information system (IMGT). In this design, the V_H-CH1 of the anti-HER2 arm is linked to the anti-CD3 scFv via a flexible G4S linker. The V_H and V_L in the scFv are connected through a flexible $(G4S)_3$ linker, which is further linked to the Fc via a G4 linker.

Stably transfected pools were generated using recombinase-mediated cassette exchange (RMCE) by co-transfecting CHO KI master cells with a targeting vector expressing the bispecific antibody and a vector expressing FLPe. The detailed procedure for creating stably transfected pools and performing production in fed-batch cultures is documented in our previous study[29]. Briefly, the stably transfected cell lines were cultured in a protein-free medium consisting of HyQ PF (GE Healthcare Life Sciences) and CD CHO (Thermo Fisher Scientific) in a 1:1 ratio. This medium was supplemented with 1 g/L sodium bicarbonate (Sigma), 6 mM glutamine (Sigma), and 0.1% Pluronic F-68 (Thermo Fisher Scientific). The cells were grown in 50 mL tubespin bioreactors (TPP), and incubated in a humidified Kuhner shaker (Adolf Kühner AG) with 8% CO_2 at 37°C. To produce the molecule, 300 mL of cell culture at a viable cell density of 3×10^5 cells/mL were inoculated into 600 mL tubespin bioreactors (TPP) under the same conditions. 30 mL of Ex-Cell Advanced CHO Feed 1 (with glucose) (SAFC, Sigma) was added on days 3, 5, 7, 9, and 11. Cell density and viability were measured on days 3, 5, 7, 9, 11, and 14 using the Vi-Cell XR viability analyzer (Beckman Coulter). The D-glucose concentration in the medium was monitored with the Nova BioProfile 100plus analyzer (Nova Biomedical). D-glucose (Sigma) was added to raise the concentration above 6 g/L if glucose levels fell below 2 g/L. The culture supernatant was collected on day 14, centrifuged, and filtered to remove cells and debris before purification.

4.3. BsAb purification

MabSelect™ PrismA resin (Cytiva) was packed into a Tricorn™ 10/150 column (Cytiva) to achieve a bed height of 15.3 cm, corresponding to a column volume (CV) of approximately 12 mL. This column was connected to an ÄKTA™ Avant 150 system (Cytiva) for the purification process. A flow rate of 153 cm/hr was maintained throughout the procedure.

The purification process began with column equilibration using 100 mM sodium phosphate, pH 7.2, 150 mM NaCl. HCCF containing less than 30 mg of monomer per mL of resin was then loaded onto the column. After loading, the column was washed with 5 CVs of the equilibration buffer to remove impurities.

Elution was carried out using 50 mM sodium citrate buffer at pH 3.6. Elution peak collection occurred between 50 mAU ascending and 50 mAU descending UV absorbance. The eluted product was immediately neutralized with 1.0 M Tris pH 8.0 buffer to reach a final product pH of 6.5. The pH values of the collected eluate and the neutralized product were measured using an external pH probe (Mettler Toledo) as necessary. Finally, the neutralized product, also known as post-ProA, was filtered through a 0.22 µm membrane prior to further use in the study.

4.4. Stress treatment conditions

The post-ProA sample was buffer-exchanged into the desired buffers using Millipore centrifugal filter units with a 30 kDa molecular weight cutoff (MWCO). The sample total protein concentration was then adjusted to 1 mg/mL for the study and incubated at 40 °C for up to 40 days.

4.5. Protein purity assessment

Protein purity was evaluated using high-performance liquid chromatography (HPLC) system (Thermo Fischer Scientific, Waltham, MA) equipped with size exclusion chromatography (SEC) (TSKgel G3000SWXL column (7.8 mm i.d. × 30 cm; Tosoh Bioscience)). The mobile phase consisted of 200 mM L-arginine, 50 mM MES, 5 mM EDTA, and 0.05% (w/w) sodium azide at pH 6.5, filtered through a 0.22 µm membrane prior to use. The protein samples were prepared at a total protein concentration of 0.25 mg/mL using 1xPBS as a diluent. 100 µL of the sample was injected onto the column, and the separation was performed at a flow rate of 0.6 mL/min. Post-column, protein purity was assessed by measuring the relative peak areas at 280 nm (A280).

4.6. Fragmentation visualization by SDS-PAGE

Non-reducing SDS-PAGE was performed using 4–15% Criterion™ TGX Stain-Free™ Protein Gels (Bio-Rad) to assess the sample purity of each fraction, following the manufacturer's instructions. Protein bands were visualized using eLuminol™ Protein Gel Stain (ABP Biosciences) with a loading of 0.3 µg protein per lane, or InstantBlue® Coomassie Protein Stain (Abcam) with a loading of 33 µg of protein to per lane.

4.7. Fragmentation analysis by mass spectrometry

Stressed Sym-bsAb samples were fractionated using the same HPLC-SEC setup as described above, but with a flow rate of 0.3 mL/min and collection of fractions at 0.6-minute intervals. Fractions of interest corresponding to elution peaks were analyzed by LC-MS as previously described[30]. Briefly, each SEC fraction was acidified with 0.3% formic acid and up to 200 ng total protein was analyzed using a TripleTOF 6600 MS (SCIEX) coupled to a nanoACQUITY UPLC (Waters) equipped with a BioResolve RP mAb Polyphenyl column (Waters). Mass spectral deconvolution was subsequently carried out using PMI-Byos v5.2.31 Intact Mass™ workflow (Protein Metrics).

Acknowledgements

This research was supported by the Bioprocessing Technology Institute (BTI), Agency for Science, Technology and Research (A*STAR).

Author contributions

Nattha Ingavat: Methodology, Validation, Formal analysis, Investigation, Data Curation, Writing - Original Draft. **Yee Jiun Kok:** Methodology, Validation, Formal analysis, Investigation, Data Curation, Writing - Original Draft. **Nuruljannah Dzulkiflie:** Formal analysis, Data Curation. **Liew Jia Min:** Formal analysis, Data Curation. **Wang Xinhui:** Formal analysis, Data Curation. **Kia Ngee Low:** Data Curation. **Ka Pui But:** Data Curation. **Amihan Anaja:** Data Curation. **Loh Han Ping:** Data Curation. **Han Kee Ong:** Data Curation. **Farouq Bin Mahfut:** Data Curation. **Yuansheng Yang:** Supervision. **Xuezhi Bi:** Conceptualization, Methodology, Investigation, Writing - Review & Editing, Supervision. **Wei Zhang:** Conceptualization, Methodology, Investigation, Resources, Writing - Review & Editing, Supervision.

Data availability statement

The datasets generated and/or analyzed during the current study are available from the corresponding author on reasonable request.

Funding details

This work was supported by the Bioprocessing Technology Institute (BTI), Agency for Science, Technology and Research (A*STAR).

Additional information

Authors declare that there are no competing financial and non-financial interests.

5. References

1. Rouet, R. and D. Christ, Bispecific antibodies with native chain structure. Nat Biotechnol, 2014. 32(2): p. 136-7.

2. Tapia-Galisteo, A., et al., When three is not a crowd: trispecific antibodies for enhanced cancer immunotherapy. Theranostics, 2023. 13(3): p. 1028-1041.

3. Wang, Q., et al., Design and Production of Bispecific Antibodies. Antibodies (Basel), 2019. 8(3).

4. Sun, Y., et al., Bispecific antibodies in cancer therapy: Target selection and regulatory requirements. Acta Pharm Sin B, 2023. 13(9): p. 3583-3597.

5. Global Bispecific Antibody Market, Drugs Sales, Patent, Price & Clinical Trials Insight 2029. 2024.

6. Bispecific Antibody Market Size, Share, Competitive Landscape and Trend Analysis Report by Product, by Applications, by End User : Global Opportunity Analysis and Industry Forecast, 2023-2032. 2023.

7. Brinkmann, U. and R.E. Kontermann, The making of bispecific antibodies. MAbs, 2017. 9(2): p. 182-212.

8. Ma, J., et al., Bispecific Antibodies: From Research to Clinical Application. Front Immunol, 2021. 12: p. 626616.

9. Chen, S.W. and W. Zhang, Current trends and challenges in the downstream purification of bispecific antibodies. Antib Ther, 2021. 4(2): p. 73-88.

10. Labrijn, A.F., et al., Bispecific antibodies: a mechanistic review of the pipeline. Nat Rev Drug Discov, 2019. 18(8): p. 585-608.

11. Wei, J., et al., Current landscape and future directions of bispecific antibodies in cancer immunotherapy. Front Immunol, 2022. 13: p. 1035276.

12. Weisser, N.E., et al., An anti-HER2 biparatopic antibody that induces unique HER2 clustering and complement-dependent cytotoxicity. Nature Communications, 2023. 14(1): p. 1394.

13. Keam, S.J., Cadonilimab: First Approval. Drugs, 2022. 82(12): p. 1333-1339.

14. Zhong, T., et al., Design of a fragment crystallizable-engineered tetravalent bispecific antibody targeting programmed cell death-1 and vascular endothelial growth factor with cooperative biological effects. iScience, 2025. 28(3): p. 111722.

15. Elshiaty, M., H. Schindler, and P. Christopoulos, Principles and Current Clinical Landscape of Multispecific Antibodies against Cancer. International Journal of Molecular Sciences, 2021. 22(11): p. 5632.

16. Nyesiga, B., et al., RUBY® - a tetravalent (2+2) bispecific antibody format with excellent functionality and IgG-like stability, pharmacology and developability properties. MAbs, 2024. 16(1): p. 2330113.

17. Bezabeh, B., et al., Insertion of scFv into the hinge domain of full-length IgG1 monoclonal antibody results in tetravalent bispecific molecule with robust properties. mAbs, 2017. 9(2): p. 240-256.

18. Loh, H.P., et al., Manufacturability and functionality assessment of different formats of T-cell engaging bispecific antibodies. MAbs, 2023. 15(1): p. 2231129.

19. Hudson, P.J. and A.A. Kortt, High avidity scFv multimers; diabodies and triabodies. J Immunol Methods, 1999. 231(1-2): p. 177-89.

20. Vlasak, J. and R. Ionescu, Fragmentation of monoclonal antibodies. MAbs, 2011. 3(3): p. 253-63.

21. Gaza-Bulseco, G. and H. Liu, Fragmentation of a recombinant monoclonal antibody at various pH. Pharm Res, 2008. 25(8): p. 1881-90.

22. Esfandiary, R., et al., Mechanism of reversible self-association of a monoclonal antibody: role of electrostatic and hydrophobic interactions. J Pharm Sci, 2015. 104(2): p. 577-86.

23. Kukic, P., et al., Coupled effect of salt and pH on proteins probed with NMR spectroscopy. Chemical Physics Letters, 2013. 579: p. 114-121.

24. Jin, Y., Y. Yi, and B. Yeung, Mass spectrometric analysis of protein deamidation – A focus on top-down and middle-down mass spectrometry. Methods, 2022. 200: p. 58-66.

25. Patel, K. and R.T. Borchardt, Chemical Pathways of Peptide Degradation. III. Effect of Primary Sequence on the Pathways of Deamidation of Asparaginyl Residues in Hexapeptides. Pharmaceutical Research, 1990. 7(8): p. 787-793.

26. Liu, H., et al., Ranking the Susceptibility of Disulfide Bonds in Human IgG1 Antibodies by Reduction, Differential Alkylation, and LC−MS Analysis. Analytical Chemistry, 2010. 82(12): p. 5219-5226.

27. Ho, S.C.L., et al., IgG Aggregation Mechanism for CHO Cell Lines Expressing Excess Heavy Chains. Molecular Biotechnology, 2015. 57(7): p. 625-634.

28. Ren, T., et al., Antibody disulfide bond reduction and recovery during biopharmaceutical process development—A review. Biotechnology and Bioengineering, 2021. 118(8): p. 2829-2844.

29. Ong, H.K., et al., Vector design for enhancing expression level and assembly of knob-into-hole based FabscFv-Fc bispecific antibodies in CHO cells. Antibody Therapeutics, 2022. 5(4): p. 288-300.

30. Ingavat, N., et al., Harnessing ceramic hydroxyapatite as an effective polishing strategy to remove product- and process-related impurities in bispecific antibody purification. Bioresources and Bioprocessing, 2023. 10(1): p. 93.

Acknowledgements

This research was supported by the Bioprocessing Technology Institute (BTI), Agency for Science, Technology and Research (A*STAR).

Author contributions

Nattha Ingavat: Methodology, Validation, Formal analysis, Investigation, Data Curation, Writing - Original Draft. **Yee Jiun Kok:** Methodology, Validation, Formal analysis, Investigation, Data Curation, Writing - Original Draft. **Nuruljannah Dzulkiflie:** Formal analysis, Data Curation. **Liew Jia Min:** Formal analysis, Data Curation. **Wang Xinhui:** Formal analysis, Data Curation. **Kia Ngee Low:** Data Curation. **Ka Pui But:** Data Curation. **Amihan Anaja:** Data Curation. **Loh Han Ping:** Data Curation. **Han Kee Ong:** Data Curation. **Farouq Bin Mahfut:** Data Curation. **Yuansheng Yang:** Supervision. **Xuezhi Bi:** Conceptualization, Methodology, Investigation, Writing - Review & Editing, Supervision. **Wei Zhang:** Conceptualization, Methodology, Investigation, Resources, Writing - Review & Editing, Supervision.

Data availability statement

The datasets generated and/or analyzed during the current study are available from the corresponding author on reasonable request.

Funding details

This work was supported by the Bioprocessing Technology Institute (BTI), Agency for Science, Technology and Research (A*STAR).

Additional information

Authors declare that there are no competing financial and non-financial interests.